

Supporting Information

Mechanically induced Gelation of a Kinetically Trapped Supramolecular Polymer

Abraham J. P. Teunissen, Marko M. L. Nieuwenhuizen, Fransico Rodríguez-Llansola, Anja R. A. Palmans
and E.W. Meijer

Email: e.w.meijer@tue.nl

Table of Contents:

Material and Methods	S2
NMR measurements	S3
FT-IR measurements	S12
Oscillatory Rheology measurements	S12
Wide Angle X-ray Spectroscopy measurements	S13
Synthetic procedures and characterization	S14
References	S18

Materials and Methods

All used solvents were of analytical grade, all chemicals were purchased from Sigma Aldrich and used without further purification. Immobilized *Candida Antarctica* Lipase B (Novozym 435) was obtained from Novozymes A/S. Unless noted otherwise all measurements were performed in chloroform. Unless noted otherwise, all gels were made by the following procedure: The compound was suspended in 1 ml of chloroform in a 32 x 11.6mm vial; this was heated until the compound was completely dissolved and then allowed to cool to room temperature. The obtained solution was then stirred for 3 hours at 900 rpm using a 6 x 1mm stirring bar, followed by a resting time of at least 2 hours.

Deconvolution of NMR spectra was performed using MestReNova software version 7.1.1-9649. All liquid NOE/ROE samples were degassed by the application of 3 freeze-pump-thaw cycles. Data processing was performed using VNMRJ.3.2.a software. All non-pulse field gradient ^1H and ^{13}C -NMR spectra were recorded on a Varian Mercury 400 MHz NMR, while all pulse field gradient measurements (i.e. NOE/ROE/DOSY) were recorded on a 500 MHz Varian Unit Inova. All NMR measurements were conducted at 25 °C. Polarized Optical Microscopy (POM) was performed on a Sondag Optische Instrumenten microscope.

NMR measurements:

Concentration dependent splitting of proton signals of **1** and **2**

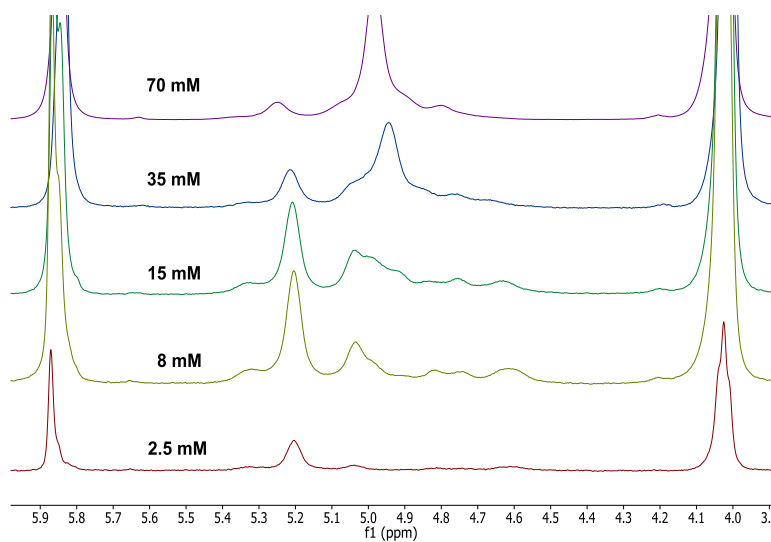


Fig. S1: Signals of urethane proton H_i of **1** at various concentrations.

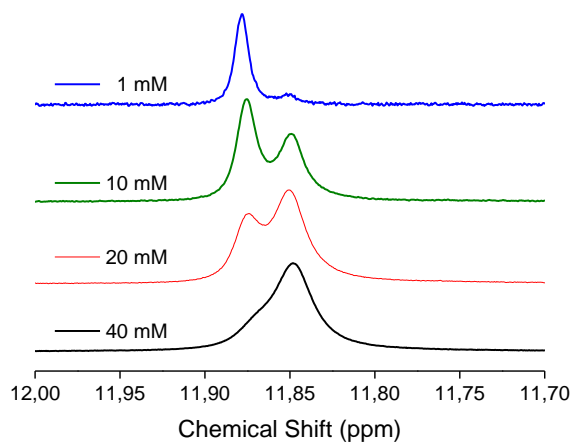


Fig. S2: Splitting of proton UPy proton H_d of **2** at various concentrations.

Concentration depended NMR spectra of both **1** and **2** reveal a splitting of proton H_d ($\approx 11,8$ ppm) into two signals. The EM corresponding to the left peak of H_d of **1** corresponds well to the EM observed for all urethane (H_i) signals associated with the monomeric cycles (Fig. 5 main text). This shows that the left

peak of proton H_d of **1** originates from the total amount of monomeric cycles. Since the same splitting is observed for H_d of **2**, it is reasonable to assume that also here the left peak represents the total of monomeric cycles of **2**. While there is no reason to assume that **2** does not form dimeric or higher order cycles, the absence of the urethane protons makes it impossible to quantify these using similar deconvolutions.

Concentration dependent behavior of various urethane signals of **1**

Since the concentration of monomeric cycles scales with the concentration of free monomer $[M]$, and the concentration of dimeric cycles with $[M]^2$, we hypothesized that by monitoring the concentration dependence of the various urethane signals of **1**, it would be possible to discriminate between the various cycles species. When plotted on a log-log plot, these should give a straight line with a slope that increases with the size of the given cycle, i.e. double the slope of the monomer for the dimeric cycles, trice the slope of the monomer for the trimeric cycles etc. Comparison of the relative integrals of the various signals revealed that signal 1, 2 and 8, display a very similar dependence on the total concentration of **1** (Fig. S3). A similar relationship was observed between peaks 3, 6, although these signals displayed a stronger concentration dependence. Unfortunately signal #7 showed an intermediate behaviour, making its assignment ambiguous. These results suggest that peak 1, 2, 8 belong to cyclic monomers, whereas peak 3 and 6 belong to cyclic dimers. The deviating concentration dependence of signal 7 might be explained by a urethane conformation that is present in both monomeric and dimeric cyclic species. Signal 4 was only observed at concentrations above ≈ 6 mM and was therefore not included in this analysis. However, the fact that it is only visible at higher concentrations, together with the relatively large size observed with DOSY (Fig. S11), suggested that it likely belongs to a dimeric or trimeric cycle.

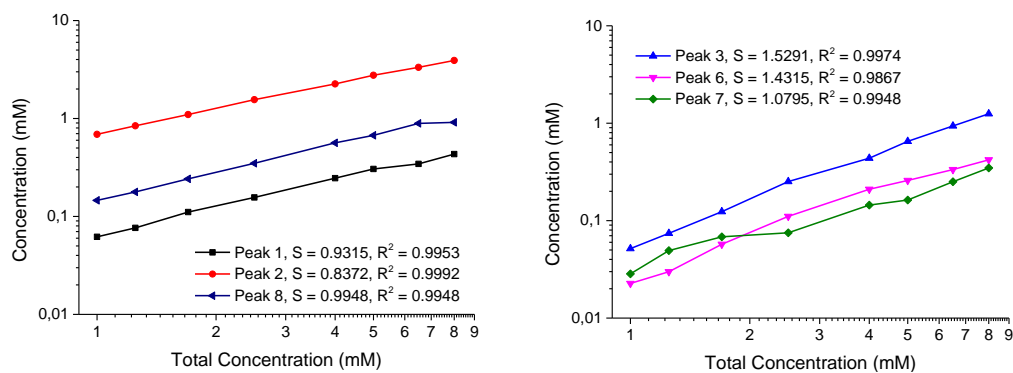


Fig. S3: Concentration dependent behaviour of various species of **1** in chloroform.

2D NOESY of the liquid state obtained after slow cooling

2D-NOESY experiments of **1** at $c = 15$ mM revealed significant exchange between nearly all urethane signals. This could originate from chemical exchange, or conformational changes within the used mixing time.

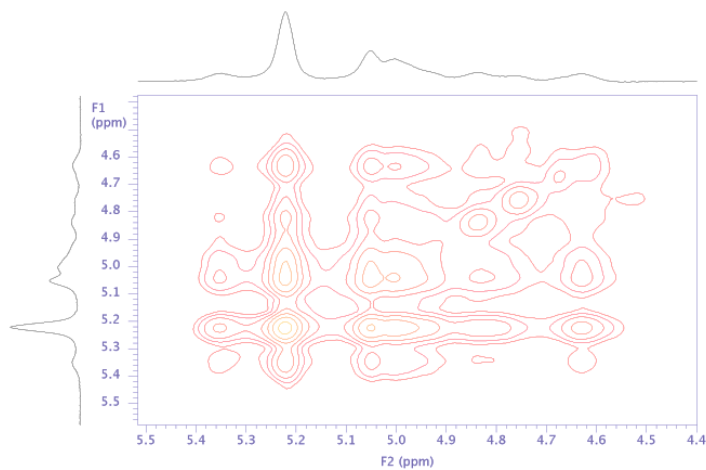


Fig. S4: Zoom of 2D-NOESY spectrum of **1** in CDCl_3 ,

$c = 15$ mM, showing the exchange between species as off-diagonal red spots.

In order to estimate the rate of chemical exchange, deuterated methanol (≈ 35 eq.) was added to the sample and the decrease in peak area was monitored over time (Fig. S5). After a period of 4 minutes, the urethane signal *Hi* had only decreased by ≈ 5 %, while other labile protons such as *Hc* and *Hd* showed a much larger decrease. This shows that the chemical exchange of proton *Hi* takes place on a times scale of minutes. Therefore the observed exchange in the NOE of **1** (mixing time = 700 ms) is almost entirely originating from conformational changes during the measurement, and demonstrates the dynamic nature of the system. Analogous experiments with deuterated ethanol or using other quantities of MeOD gave similar results.

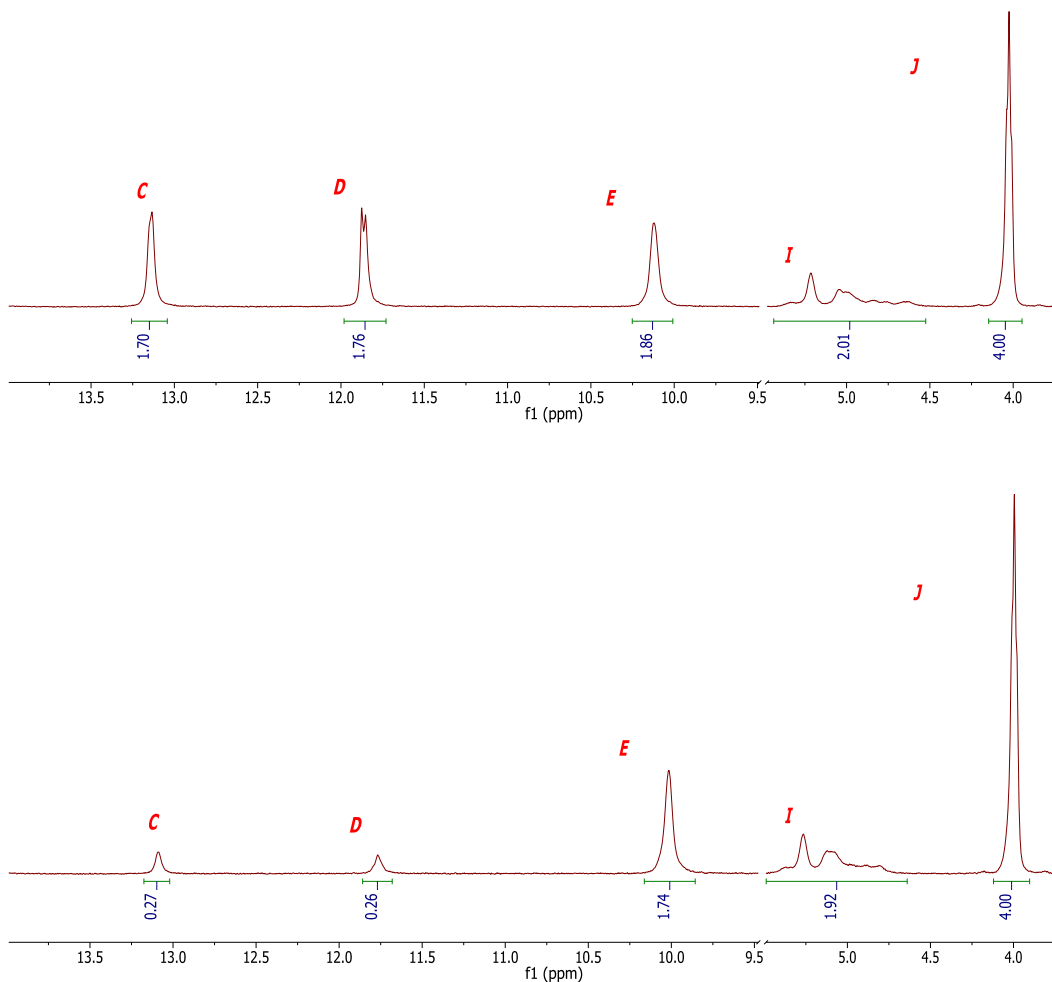


Fig. S5: Upper frame: ^1H -NMR spectra of **1** $c = 15$ mM before addition of MeOD.

Lower frame: ^1H -NMR spectra of **1** $c = 15$ mM 4 minutes after addition of 15 μL MeOD to 0.7 mL sample.

DPFGSE-NOESY of the cyclic species in the slowly cooled solution

c = 2.5 mM solution

Mixing time = 1000ms

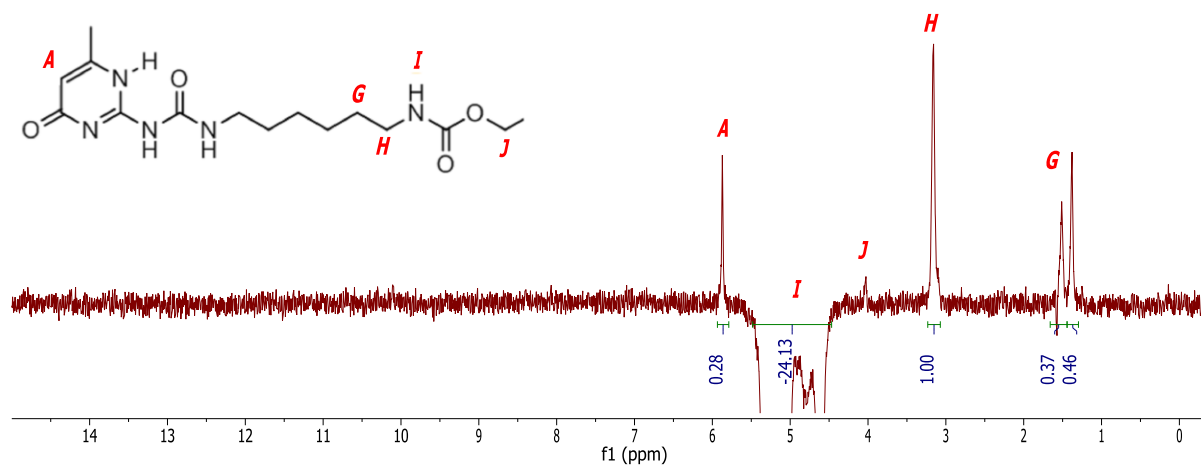


Fig. S6: NOESY spectra of **1** c = 2.5 mM, excited at proton *Hi*.

DPFGSE-ROESY selective excitation of signal #5 (linear polymers) in the slowly cooled solution

For unknown reasons the spinning interfered with the NOESY measurements, therefore a similar ROESY sequence was used for the measurements on the 60 mM solution and gel.

Mixing time = 600 ms, Spinning Speed = 2000 rpm

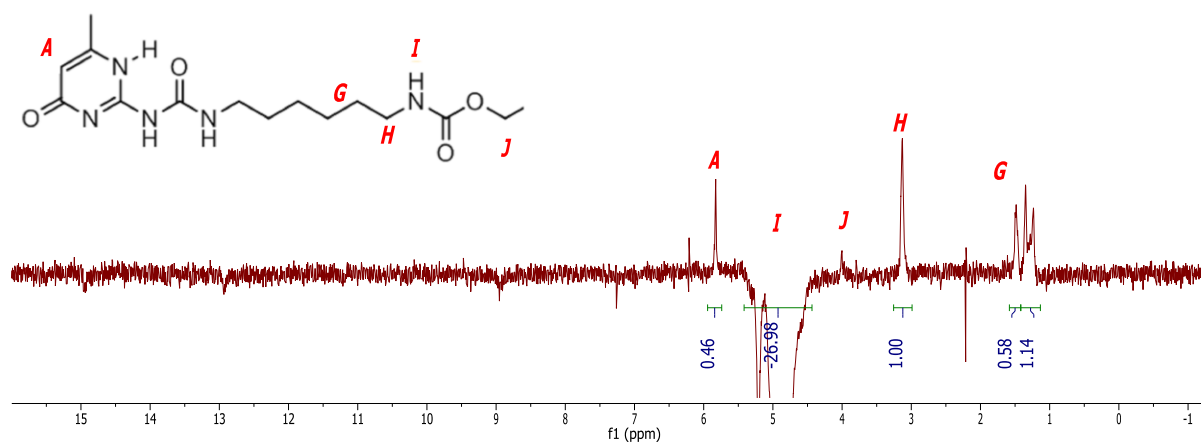


Fig. S7: DPGSE-ROESY spectra of **1** in solution $c = 60$ mM, excited at the signal of proton Hi , corresponding to the linear polymers.

DPFGSE-ROESY $c = 60$ mM Gel

Mixing time = 600 ms, Spinning Speed = 2000 rpm

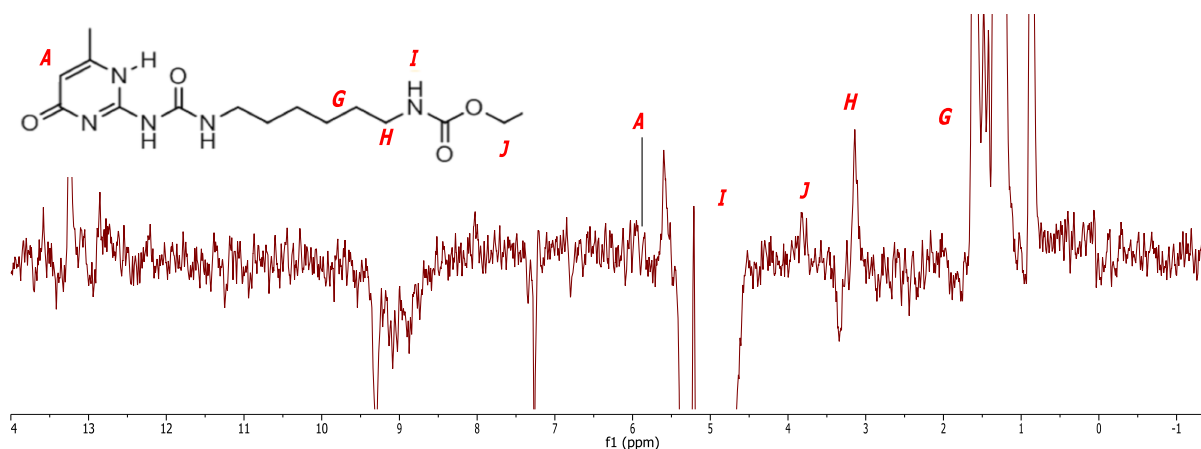


Fig. S8: ROESY spectra of **1** in a gel $c = 60$ mM, while all Hi signals were excited. “A” denotes the position of proton Ha in the ^1H -NMR spectrum of the gel.

As depicted above the NOE contact between protons Hi and Ha seems absent or is significantly weaker than in the solution at the same concentration (the NOE intensity of Hh is used as a reference). All other positive and negative signals have been successfully identified as spinning sidebands.

Distance determination by NOESY:

As described by Butts *et al*^{S1}, within a given experiment the relative intensity of the NOE signals of a pair of protons (H_x & H_y) is related to their relative distance to the excited proton (H_z) by the following equation:

$$\frac{\eta_{Hx}}{\eta_{Hy}} = \frac{r_{Hx-Hz}^{-6}}{r_{Hy-Hz}^{-6}}$$

Similar analysis of our NOE and molecular dynamics results resulted in very similar distances.

Distance analysis from NOE data of **1** at $c = 2.5$ mM

$$\frac{\eta_{Ha}}{\eta_{Hh}} = \frac{0.28}{0.50} = \frac{r_{Ha-Hi}^{-6}}{r_{Hh-Hi}^{-6}}$$

$$\frac{r_{Ha-Hi}}{r_{Hh-Hi}} = \mathbf{1.101}$$

(Since the signal of Hh is resulting from two protons its integral is divided by two)

Distance estimation based on molecular dynamics simulation of the cyclic monomer

$$r_{Ha-Hi} = 2.97 \text{ \AA}$$

$$r_{Hh-Hi} = \frac{2.98 + 2.38}{2} = 2.68 \text{ \AA}$$

$$\frac{r_{Ha-Hi}}{r_{Hh-Hi}} = \frac{2.97}{2.68} = \mathbf{1.108}$$

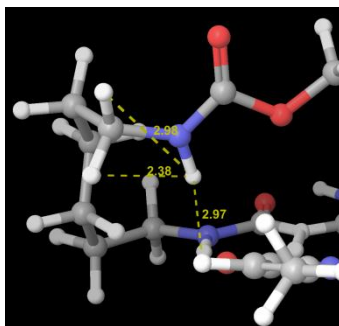


Fig. S9: Zoom of the minimized structure of the monomeric cycle of **1**.

Fitting of DOSY results of 1 at c = 15 mM

To get further insight in the nature of the different species a detailed DOSY analysis was performed. To rule out the influence of peak overlap on the resulting diffusion coefficients, all gradient depended spectra obtained during the measurement were deconvoluted before being fitted with the Stejskal-Tanner equation.^{S2}

$$A = A_o * \exp[(G\gamma_H\delta)^2 * D * (\Delta - \frac{\delta}{3} - \frac{\tau}{2})]$$

Δ = relaxation delay = 30 ms

γ_H = ^1H gyromagnetic ratio = $267.513 \cdot 10^6 \text{ rad s}^{-1} \text{ T}^{-1}$

D = diffusion coefficient

δ = pulse duration = 3.5 ms

τ = gradient stabilization delay = 2.5 ms

G = gradient strength = $g_z * g_{cal}$

$g_z = 1130 \text{ to } 22500$

$g_{cal} = 0.0001906$

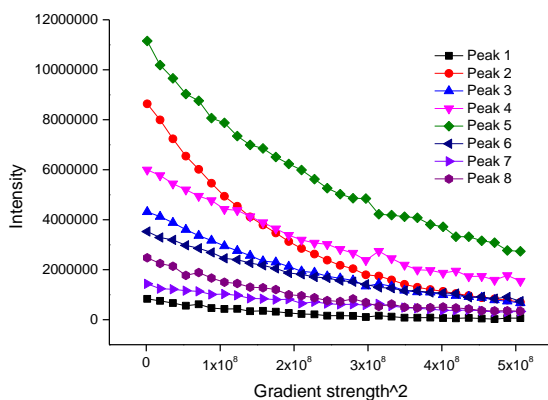


Fig. S10: Exponential decay of signals 1 to 8 as a function of gradient strength.

The calculated diffusion coefficients were corrected for the observed change in the self-diffusion of CHCl_3 .^{S3}

$$D = D_{meas} * D_{pure}^{sol} / D_{meas}^{sol}$$

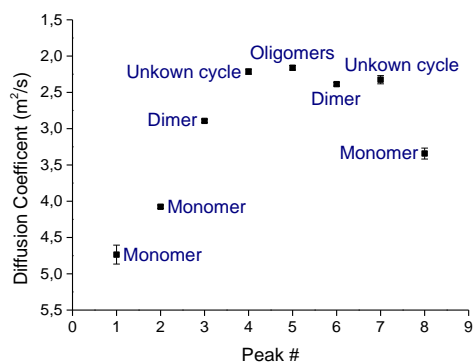


Fig. S11: DOSY spectra of all urethane signals of **1**, and their identification according to concentration dependent behaviour as shown in Fig. S3, $c = 15$ mM.

As expected from the results displayed in Fig. S3, the DOSY results show that the species attributed to the monomer have the highest diffusion coefficient, followed by the dimeric and the linear chains respectively. The relatively large difference in diffusion coefficient between different conformational isomers might be the result of a different orientation of the linker with respect to the UPy dimer.

FT-IR measurements:

All infrared measurements were performed on a Perkin Elmer FT-IR Spectrum Two apparatus. While the gel was measured in ATR mode, the liquid (CHCl_3) samples were measured using a 0.05 mm NaCl cell.

Oscillatory Rheology measurements:

Rheology measurements were performed on a Anton Paar Physica MCR 501 apparatus, using a 25 mm parallel plate setup (PP25). To minimize evaporation of solvent, the measurements were performed at 10 °C in a solvent saturated atmosphere. Since evaporating seemed most significant during loading of the sample, the gels were prepared using 2 ml sample in a 45 x 27 mm vial for easy transfer. Besides this, the same gelation procedure as mentioned in the material and methods section was used.

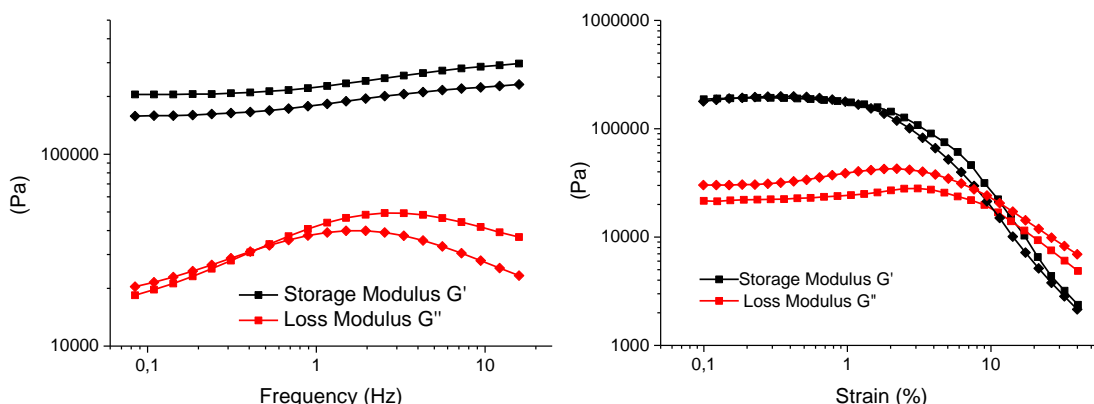


Fig. S12: Left: frequency sweep measurement of **1**, Right: strain sweep measurement of **1**.

Frequency sweep was obtained with a strain of $\gamma = 1\%$. Strains sweep was obtained with a frequency of $\omega = 1$ rad/s. The concentration of both samples was 80 mM. The measurements were performed in duplo after loading of a fresh sample, the squares depicted results from measurement one, the circles depicted results from measurement two. The peak in the Loss Modulus is likely related to relaxation of the UPy-UPy bonds, which takes place on similar

timescales (≈ 0.12 s).^{S4}

Wide Angle X-Ray Scattering (WAXS):

Strong gels were dried *via* a gentle air flow ($c = 80$ mM). X-Ray scattering measurements were performed on a Ganesha lab instrument equipped with a GeniX-Cu ultra-low divergence source producing X-ray photons with a wavelength of 1.54 \AA and a flux of 1×10^8 ph/s. Scattering patterns were collected using a Pilatus 300K silicon detector with 487×619 pixels of 172 \mu m^2 in size, at a sample-to detector distance of 350 mm. The beam center and the q range were calibrated using the diffraction peaks of silver behenate. The samples were measured in-between micca plates. While the large increase in concentration during drying doesn't seem to affect the strong gels, the weak gels immediately turned into non-transparent gels with similar appearance as the strong gels, for this reason they were not further analyzed using WAXS.

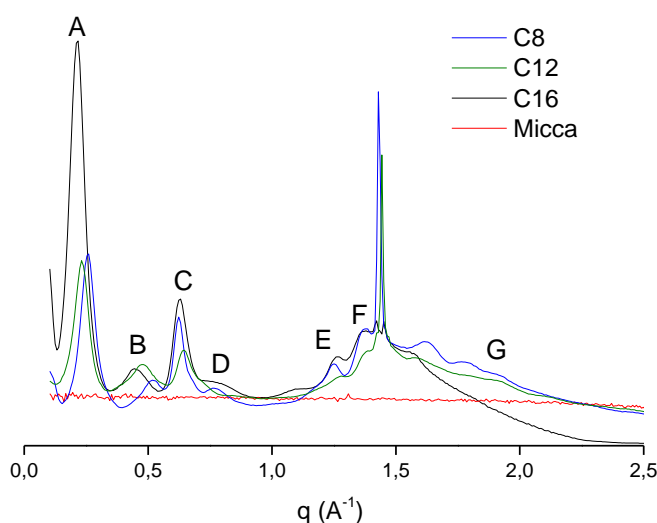


Fig. S13: WAXS results on dried gels of **1** with C_{12} spacer and similar compounds with C_8 and C_{16} spacers between the urethanes.

Distances corresponding to the peaks found for the molecule with C_{12} spacer (i.e. **1**).

A 27.2 \AA Attributed to the total length of the UPy-UPy linker

B 13.06 \AA Attributed to the in-chain urethane-urethane distance

C 9.94 \AA 11.05 \AA is reported for UPy stack-stack distances^{S5}

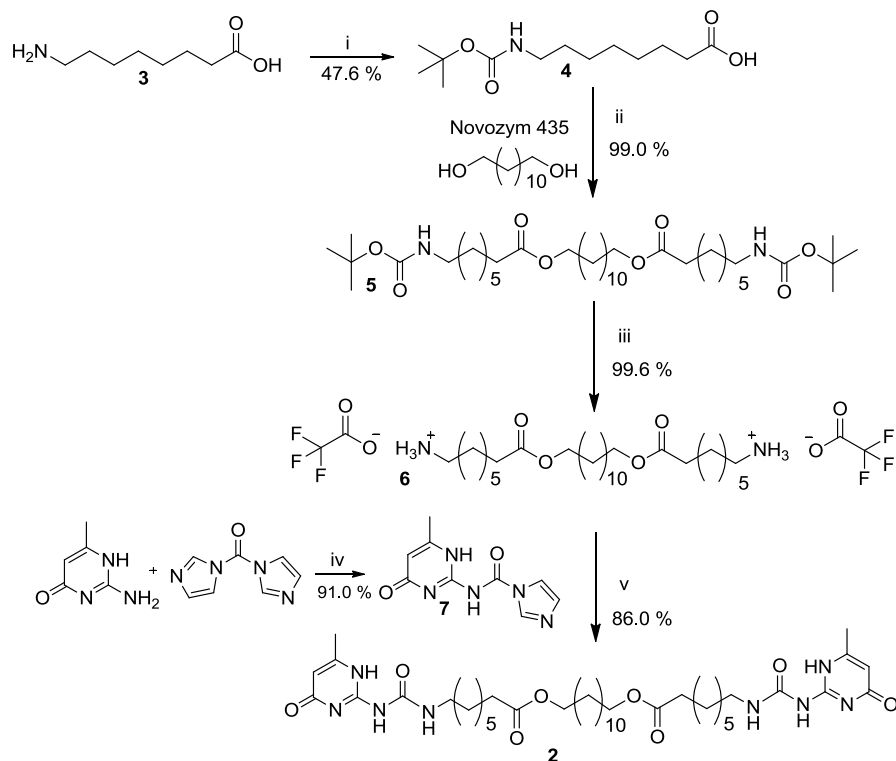
D 8.16 \AA Attributed correspond to UPy-urethane distance

E 5.03 \AA 5.05 \AA is reported for urethane-urethane hydrogen bond distances in a polyurethane^{S6}

F 4.55 \AA 4.56 \AA is reported for UPy stack-stack distances^{S5}

G 3.32 \AA $3.5\text{-}4.0 \text{ \AA}$ is reported for benzene and naphthalene pi-pi stacking^{S7}

Synthetic Procedures and Characterization:



Scheme S1: Synthetic route towards compound **2**

Reagents and conditions: i) DCM, H₂O, NaOH, di-*tert*-butyl dicarbonate, RT; ii) hexane, Novozyme 435, 70 °C, 800 mbar; iii) DCM, TFA, RT; iv) DMSO, 80 °C; v) DMF, triethylamine, RT.

8-((*tert*-Butoxycarbonyl)amino)octanoic acid (**4**)

8-Aminooctanoic acid (3.0 g, 18.8 mmol) was dissolved in a mixture of DCM (5 mL) and water (5 mL). NaOH (1.5 g, 37.5 mmol) was added and the solution was cooled to 0 °C. A solution of di-*tert*-butyl dicarbonate (4.1 g, 18.8 mmol) in DCM (20 mL) was slowly added and the reaction mixture was stirred for 24 h at room temperature. The solution was acidified using conc. HCl (3 mL) and the aqueous phase was extracted with DCM (2 x 40 mL). The combined organic phases were dried using MgSO₄ and the solvent was removed under vacuum. Yield: 2.32 g, 8.97 mmol. η : 47.6 %. ¹H NMR δ (400 MHz; CDCl₃): 9.2 (1H, bs, COOH), 4.54 (1H, s, NH), 3.09 (2H, m, NH-CH₂), 2.33 (t, CO-CH₂), 1.66 (NH-CH₂-CH₂), 1.44 (11H, m, CH₃, CH₂), 1.32 (6H, m, CH₂). ¹³C NMR δ (100 MHz, CDCl₃): 179.12, 155.99, 79.10, 40.53, 33.95, 29.93, 28.92, 28.40, 26.53, 24.58. MALDI-TOF-MS: Calc. Mass 259.18 g/mol, Found 282.27 g/mol (M+Na)⁺.

Dodecane-1,12-diyl bis(8-((*tert*-butoxycarbonyl)amino)octanoate) (5)

8-((*tert*-Butoxycarbonyl)amino)octanoic acid (142 mg, 0.548 mmol) and dodecane-1,12-diol (55 mg, 0.272 mmol) were dissolved in hexane (5 mL) and Novozym 435 beads (15 mg) were added. The solution was put on a rotary evaporator and gently rotated for 3 h at 70 °C at a pressure of 800 mbar. When necessary, extra hexane was added. The solution was cooled down, hexane (20 mL) was added and the enzyme beads were filtered off and rinsed with additional hexane. The solvent was evaporated under vacuum to yield the desired compound. Yield: 185 mg, 0.27 mmol. η : 99 %. ^1H NMR δ (400MHz; CDCl_3): 4.48 (2H, bs, NH), 4.05 (4H, t, O-CH₂), 3.11 (4H, m, N-CH₂), 1.62 (8H, m, CH₂), 1.44 (22H, m, CH₃, CH₂), 1.31 (28H, m, CH₂). ^{13}C NMR δ (100 MHz, CDCl_3): 173.89, 155.97, 79.02, 64.41, 40.52, 34.31, 30.00, 29.53, 29.50, 29.24, 29.03, 28.91, 28.64, 28.42, 26.60, 25.91, 24.88. MALDI-TOF-MS: Calc. Mass 684.53 g/mol, Found 707.53 g/mol ($\text{M}+\text{Na}$)⁺.

8,8'-(Dodecane-1,12-diylbis(oxy))bis(8-oxooctan-1-aminium) 2,2,2-trifluoroacetate (6)

Dodecane-1,12-diyl bis(8-((*tert*-butoxycarbonyl)amino)octanoate) (193 mg, 0.28 mmol) was dissolved in a solution of 30 % TFA in DCM (10 mL total). The mixture was stirred at room temperature for 3 h. The solvents were co-evaporated with toluene (2 x 5 mL) to yield the desired product. Yield: 137 mg, η : 99.6 %. ^1H NMR δ (400MHz; CDCl_3): 7.86 (6H, bs, NH_3^+), 4.09 (4H, t, O-CH₂), 2.98 (4H, bs, N-CH₂), 2.32 (4H, t, C=O-CH₂), 1.75-1.54 (12H, m, CH₂), 1.47-1.21 (28H, m, CH₂). ^{13}C NMR δ (100 MHz, CDCl_3): 174.38, 67.06, 39.95, 34.23, 29.51, 29.05, 28.83, 28.42, 28.32, 27.25, 25.72, 24.56. MALDI-TOF-MS: Calc. Mass 684.99 g/mol, Found 486.46 g/mol (Monoprotonated diamine without TFA).

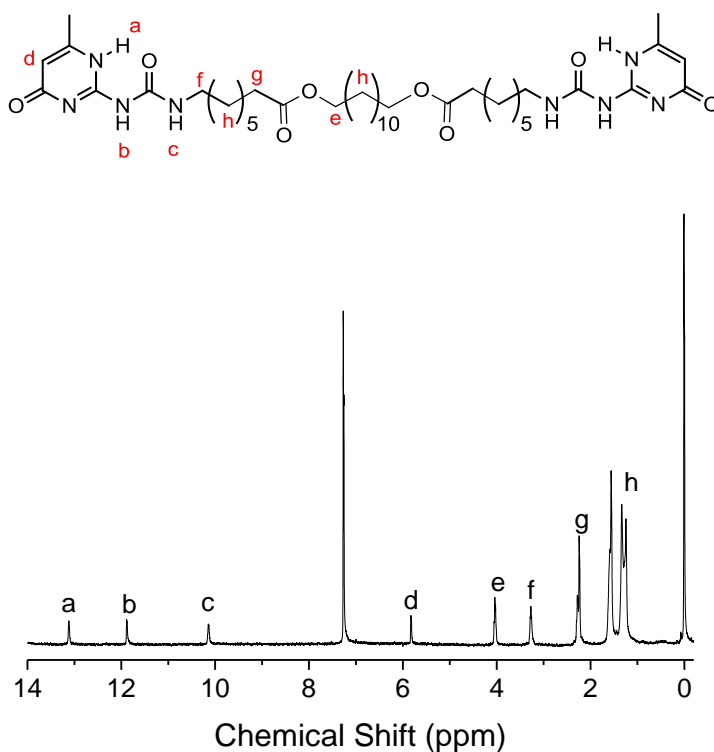
N-(6-Methyl-4-oxo-1,4-dihydropyrimidin-2-yl)-1H-imidazole-1-carboxamide (7)

2-Amino-6-methylpyrimidin-4(1*H*)-one (1.0 g, 7.99 mmol) was dissolved in DMSO (10 mL), di(1*H*-imidazol-1-yl)methanone (1.68 g, 10.36 mmol) was added and the mixture was stirred for 24 h at 80 °C. The solution was cooled to room temperature and acetone was added to precipitate the product. The precipitate was filtered and the residue washed with acetone. The product was dried under vacuum to yield the desired product. Yield: 1.59 g, 7.25 mmol. η : 91%. Remark: Due to its extremely low solubility in most solvents this compound is hard to characterize. IR (ATR): $\tilde{\nu}$ = 3175, 3075, 2648 (bs) 1701, 1645, 1601, 1509, 1479, 1375, 1334, 1320, 1276, 1233, 1224, 1190, 1169, 1090, 1065, 1026, 983 cm^{-1} .^{S7}

Dodecane-1,12-diyl bis(8-(3-(6-methyl-4-oxo-1,4-dihydropyrimidin-2-yl)ureido)octanoate) (2)

8,8'-(Dodecane-1,12-diylbis(oxy))bis(8-oxooctan-1-aminium) 2,2,2-trifluoroacetate (137 mg, 0.28 mmol) was dissolved in DMF (10 mL). Triethylamine (0.2 mL) and *N*-(6-methyl-4-oxo-1,4-dihydropyrimidin-2-yl)-1*H*-imidazole-1-carboxamide (300 mg, 1.37 mmol) were added and the mixture was stirred at room temperature for 24 h. The solvent was removed *in vacuo* and chloroform (50 mL) was added. The organic phase was filtered and subsequently dried under vacuum to yield the desired compound. Yield: 191 mg, 0.243 mmol. η : 86 %. ^1H NMR δ (400MHz; CDCl_3): 13.11 (2H, s, $\text{CH}_3\text{CN-H}$), 11.88 (2H, s, $\text{CH}_2\text{NH}(\text{C=O})\text{NH}$), 10.11 (2H, s, $\text{CH}_2\text{NH}(\text{C=O})\text{NH}$), 5.81 (2H, s, $\text{CH}=\text{CCH}_3$), 4.05 (4H, t, $(\text{C=O})\text{O-CH}_2$), 3.25 (4H, m, NH-CH_2), 2.22 (6H, m, CH_3), 1.54 (6H, m, CH_3), 1.55-1.20 (40H, m, CH_2). ^{13}C NMR δ (100 MHz, CDCl_3): 173.92, 172.99, 156.57, 154.70, 148.16, 106.70, 64.31, 39.97, 34.34, 29.53, 29.23, 28.64, 26.41, 25.97, 24.83, 18.93. MALDI-TOF-MS: Calc. Mass 786.50 g/mol, Found 787.52 g/mol ($\text{M}+\text{H}$) $^+$.

^1H - and ^{13}C -NMR spectra of 2



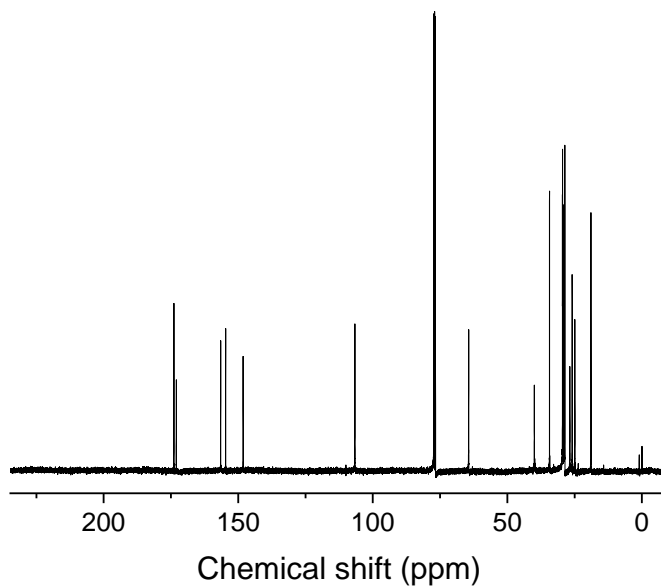


Fig. S14: Upper frame: Structure of **2**; Middel frame: ^1H -NMR of **2**; Lower frame: ^{13}C -NMR of **2**.

References

- S1 C. P. Butts, C. R. Jones, E. C. Towers, J. L. Flynn, L. Appleby and N. J. Barron, *Org. & Biomol. Chem.*, 2011, 9, 177.
- S2 E. O. Stejskal and J. E. Tanner, *Chem. Phys.*, 1965, 42, 288.
- S3 V. G. H. Lafitte, A. E. Aliev, P. N. Horton, M. B. Hursthouse and H. C. Hailes, *Chem. Commun.*, 2006, 2173.
- S4 S. H. M. Sontjes, R. P. Sijbesma, M. H. P. van Genderen, E. W. Meijer, *J. Am. Chem. Soc.*, **2000**, 122, 7487-7493.
- S5 J. L. Wietor, D. J. M. van Beek, G. W. Peters, E. Mendes and R. P. Sijbesma, *Macromolecules*, 2011, 44, 1211.
- S6 J. Blackwell, M. R. Nagarajan and T. B. Hotink, *Polymer*, 1981, 22, 1534.
- S7 T. Sato, T. Tsuneda and K. J. Hirao, *J. Chem. Phys.*, 2005, 123, 104307.
- S8 P. Y. Dankers, P. J. H. M. Adams, D. W. P. M. Löwik, J. C. M. van Hest and E. W. Meijer, *Eur. J. Org. Chem.*, 2007, 3622.